RSC Advances

PAPER

View Article Online
View Journal | View Issue

Cite this: *RSC Adv.*, 2020, **10**, 8198

Biocorrosion of pure and SLA titanium surfaces in the presence of *Porphyromonas gingivalis* and its effects on osteoblast behavior

Li-na Xu,†[ab] Xiao-yu Yu,†[ab] Wan-qing Chen,[ab] Song-mei Zhang[c] and Jing Qiu *[ab]

Objective: The study aims to investigate the biocorrosion behavior of *Porphyromonas gingivalis* on pure and SLA titanium surfaces and its effects on surface characteristics and osteoblast behavior. *Methods*: Pure and SLA titanium specimens were immersed in culture medium with *P. gingivalis* and incubated for 7 days. *P. gingivalis* colonization on the pure and SLA titanium surfaces was observed by scanning electron microscopy (SEM). The pure and SLA titanium surface characteristics were analyzed *via* X-ray photoelectron spectroscopy (XPS), surface roughness and surface wettability. The corrosion behaviors of pure and SLA titanium specimens were evaluated by electrochemical corrosion test. The osteoblast behavior of MC3T3-E1 cells on the pure and SLA titanium surfaces after *P. gingivalis* colonization was investigated by cell adhesion and western blot assays. *Results*: *P. gingivalis* colonized on the pure and SLA titanium surfaces was observed by SEM. The XPS analysis demonstrated reductions in the relative levels of titanium and oxygen and obvious reductions of dominant titanium dioxide (TiO_2) on both titanium surfaces after immersing the metal in *P. gingivalis* culture. In addition, their roughness and wettability were changed. Correspondingly, the electrochemical corrosion test results revealed significant decreases in the corrosion resistance and increases in the corrosion rate of the pure and SLA titanium specimens after immersion in *P. gingivalis* culture. The results of the *in vitro* study showed that the pre-corroded pure and SLA titanium surfaces by *P. gingivalis* exhibited lower osteocompatibility and down-regulated the adhesion, spreading and osteogenic differentiation abilities of MC3T3-E1 cells. *Conclusions*: *P. gingivalis* was able to colonize on the pure and SLA titanium surfaces and weaken their surface properties, especially a decrease in the protective TiO_2 film, which induced the biocorrosion and further negatively affected the osteoblast behavior.

Received 7th January 2020
Accepted 20th February 2020

DOI: 10.1039/d0ra00154f

rsc.li/rsc-advances

1. Introduction

Pure titanium and its alloys are the first option for applications in implant dentistry, because of brilliant biocompatibility, corrosion resistance, and mechanical property.[1] And rough titanium surfaces have been established to be more suitable for osteoblast growth than smooth titanium surface.[2,3] Sand-blasting with large grit and acid etching (SLA) is one of the most widespread surface treatments for dental implants, and this special hierarchical structure contributes to high osteoconduction and clinical success rates.[4,5]

Titanium is a material with good chemical stability and high corrosion resistance compared with other metallic materials owing to a compact titanium dioxide (TiO_2) film on its surface, which forms in oxygen containing environments spontaneously.[6] Although much research has demonstrated that the protective TiO_2 layer is stable on the titanium surface,[7,8] the disintegration of the TiO_2 layer may occur in the complicated oral environment that includes saliva, foodstuffs, toothpaste, mouthwash, and microbes.[9] These agents can induce the corrosion or biodegradation of metals due to their thermal, ionic, and microbiological properties.[10] Corrosion of the titanium surface may accelerate the release of titanium ions, which have detrimental influence on implant osteointegration. The surfaces of failed titanium implants present clear signs of localized corrosion on the implant and its abutment.[11] While the corrosion behavior of dental implant is related to various factors, the most notable one is bacterial adhesion to the implant surface, with the subsequent formation of a microbial film that further influences the titanium surface functionality.[12,13]

[a]*Department of Oral Implantology, Affiliated Hospital of Stomatology, Nanjing Medical University, Nanjing, 210029, PR China. E-mail: qiujing@njmu.edu.cn; Tel: +86 25 69593084*

[b]*Jiangsu Key Laboratory of Oral Disease, Nanjing Medical University, Nanjing, PR China*

[c]*Department of General Dentistry, Eastman Institute for Oral Health, University of Rochester, Rochester, NY, USA*

† These authors contributed equally to this work.

When considering the factors of implant failure, research on the corrosion behavior of titanium surfaces upon exposure to microorganisms has been the focus, due to the complex variety of microorganisms and corrosive matter in the oral microenvironment.[6] *Porphyromonas gingivalis* (*P. gingivalis*), a member of the human oral flora, is considered to be the main pathogen of human periodontitis.[14] Furthermore, it had been detected at higher number from microbial films around implants in patients with peri-implantitis.[15,16] And *P. gingivalis* had been found to attach on titanium surfaces in large amounts during the process of biofilm formation on titanium surfaces.[17,18] Meanwhile, *P. gingivalis* has several virulence factors like lipopolysaccharides (LPS) and releases volatile sulfur compounds (VSCs) as a result of its metabolism, which can potentially promote titanium corrosion.[16]

Biocorrosion on the titanium surface may damage the oxide layer and influence the titanium surface energy or surface chemical characteristics.[19] Carlen *et al.*[20] reported that bacterial corrosion could roughen the metal surface, and a rough metal surface became more conducive to bacterial adhesion. This result closely paralleled the findings of our previous studies, which demonstrated that *S. mutans* could enhance the corrosion behavior of the dental alloys and the presence of corroded alloy surfaces up-regulated the virulent gene expression in *S. mutans*.[21] Barão *et al.*[19] reported the increased attachment of *P. gingivalis* to pre-corroded commercially pure titanium (cpTi) and Ti–6Al–4V alloy in artificial saliva solution with different pH values. Our previous study has found that the metabolites, produced by *A. naeslundii*, could weaken the integrity and stability of the protective TiO_2 in surface oxides and then enhance the corrosion behavior of pure titanium.[22] Furthermore, the results of recent studies confirmed the negative effect of bacterial colonies, such as *S. mutans*, on the corrosion resistance of titanium and its alloys.[6,23]

Regarding the *P. gingivalis*, however, few studies are available in literature demonstrating its impacts on surface properties and corrosion behavior of titanium implant at present. Based on the above considerations, the novelty of this work is to explore the biocorrosion of different titanium surfaces upon exposure to *P. gingivalis* and its further effects on osteoblast behavior. The research hypothesis was that the colonization of *P. gingivalis* on titanium might weaken its surface oxide film, which might induce the biocorrosion and further negatively affected the osteoblast behavior.

2. Materials and methods

2.1. Specimen preparation

Square specimens of commercially pure titanium (Grade 4, 99.5 wt% purity, Alfa Aesar, USA) with dimension of 4 mm × 4 mm × 0.25 mm were ground with a series of SiC papers (800, 1000, 1200, and 1500 grit), and then ultrasonically cleaned in ethanol and distilled water for 5 minutes before being dried at 65 °C in an oven. Next, the SLA titanium surface was acquired by sandblasting with alumina particles, followed by etching with a solution including HF/HNO_3 for 10 minutes at room temperature and a solution containing HCl/H_2SO_4 for 30 minutes in a water bath at 80 °C. Subsequently, all specimens, including pure and SLA titanium surfaces, were ultrasonically cleaned, as described above, disinfected in an autoclave for 15 minutes at 121 °C prior to use, and finally dried in an oven for 24 hours at 65 °C.

2.2. *P. gingivalis* biofilm formation and incubation

P. gingivalis (ATCC 33277) was cultured in brain heart infusion (BHI) (Oxiod Co., Ltd., England) broth containing 0.001% hemin (Dulai biological Co., Ltd., Nanjing, China) and 0.0001% vitamin K1 (Aladdin Co., Ltd., Shanghai, China) in an anaerobic chamber (10% H_2, 5% CO_2, and 85% N_2, RUskinn Bugbox Co., Ltd., England) at 37 °C. For attachment assay, 1×10^8 colony-forming units (CFU) mL^{-1} of *P. gingivalis*, evaluated with a bacterial turbidity meter (WGZ-2XJ, XinRui Co., Ltd., Shanghai, China), were used to inoculate for all specimens. The pure and SLA titanium specimens for experimental groups were placed in 12-well plates with each well containing BHI for 3 mL, then inoculated with *P. gingivalis*, and denoted as Ti-pg and SLA-pg specimens. The pure and SLA titanium specimens for control groups were incubated in BHI only and denoted as Ti and SLA specimens. The main components of BHI are as following: beef heart infusion solids 17.5 g L^{-1}, proteose peptone 10.0 g L^{-1}, glucose 2.0 g L^{-1}, NaCl 5.0 g L^{-1}, Na_2HPO_4 2.5 g L^{-1}. All plates were incubated in an anaerobic chamber (80% N_2, 10% H_2, 10% CO_2) for 7 days. The medium was renewed every two days.

2.3. Surface characterization

The growth condition of the bacteria upon the pure and SLA titanium surfaces was observed by scanning electron microscopy (SEM). In order to achieve microscopic analysis, different titanium specimens with and without biofilms were cleaned by phosphate-buffered saline (PBS), and then fixed in 2% glutaraldehyde for 30 minutes. Afterwards, the specimens were rinsed in PBS and dehydrated through a series of graded ethanol solutions (30, 50, 70, and 90%) for 10 minutes. Finally, the specimens were dehydrated using anhydrous ethanol and sputter-coated with gold before SEM (Sirion 200, Philips, Eindhoven, Netherlands) observation.

X-ray photoelectron spectroscopy (XPS) was utilized to analyze elemental components and their chemical states on different titanium specimens with and without biofilms. Before testing, the specimens were ultrasonically washed to clear the biofilms in deionized water, ethanol, and deionized water each for 5 minutes. XPS was performed (Thermo Scientific Escalab 250Xi, USA) using an Al Kα radiation at 15 kV and 150 W. Survey and high-resolution spectra were obtained using pass energies of 160 and 40 eV. Reference binding energy of each element was obtained from the National Institute of Standards and Technology XPS Online Database (http://srdata.nist.gov/xps/). Spectral features were compared to the C 1s binding energy signal to 284.8 eV. Quantitative analysis of surface composition was obtained from the peak areas and atomic sensitivity factors.

After clearing the biofilms as above, the surface roughness and three-dimensional images of specimens were measured

with an optical profilometer (MicroXam™, Phase-Shift, UP, Rtec Co, USA). The scanning area of each specimen was 50 μm × 50 μm. All measurements were performed in triplicate. The surface wettabilities of specimens were examined from the contact angle *via* testing a droplet of pure water on the specimens by an Automatic Contact Angle Meter Model SL200B (Kenuo, USA) in an ambient environment. All tests were conducted in quintuplicate.

2.4. Electrochemical corrosion test

After clearing the biofilms as above, each specimen was mounted in self-cured epoxy resin carefully to expose its test surface area of 4 mm × 4 mm. Corrosion tests were carried out using an electrochemical potentiostat (CS310H, Corrtest Instruments Co., Ltd., Wuhan, China) *via* a test cell with the mounted specimen as the working electrode, a high-purity platinum wire as the counter electrode, and Ag/AgCl as the reference electrode. Corrosion tests were performed in triplicate for each group in Hank's solution (Gibco, Life Technologies, Carlsbad, CA, USA) at 37 ± 0.5 °C. The main components of Hank's solution are as following: NaCl 8.0 g L^{-1}, KCl 0.4 g L^{-1}, $NaHCO_3$ 0.35 g L^{-1}, $NaH_2PO_4 \cdot H_2O$ 0.25 g L^{-1}, $Na_2HPO_4 \cdot 2H_2O$ 0.06 g L^{-1}, $MgCl_2$ 0.19 g L^{-1}, $MgSO_4 \cdot 7H_2O$ 0.06 g L^{-1}, $CaCl_2 \cdot 2H_2O$ 0.19 g L^{-1}, glucose 1.0 g L^{-1}. Each specimen was permitted to gain a stable open circuit potential (OCP) for 2 hours, after which a 10 mV amplitude sine wave potential was employed through a frequency range from 1000 kHz to 10 mHz. The electrochemical impedance spectroscopy (EIS) tests were applied using dedicated Corrtest software (CS Studio 5, Corrtest Instruments Co., Ltd., Wuhan, China). The achieved data, including Nyquist plot, Bode $|Z|$, and Bode phase diagrams, were analyzed and fitted using an appropriate equivalent circuit by the ZsimpWin software. After that, the potentiodynamic polarization test was initiated within a scanning range from −800 mV to 3000 mV (*vs.* reference electrode) at a sweep rate of 2 mV s^{-1}. The acquired polarization curves were analyzed using curve-fitting routine of the dedicated Corrtest software to determine the corrosion potential (E_{corr}), corrosion current (I_{corr}) and corrosion rate.

2.5. Cell culture

An osteoblast-like cell line, MC3T3-E1 cells, obtained from the Cell Bank of Chinese Academy of Sciences (Shanghai, China), was chosen to act as an *in vitro* model of osteoblast development. The MC3T3-E1 cells were cultured in alpha-minimum essential medium (α-MEM; Gibco, Life Technologies, Carlsbad, CA, USA) containing 10% fetal bovine serum and 1% penicillin/streptomycin in a humidified atmosphere of 5% CO_2 and 95% air at 37 °C. The cells were passaged when covering 80% area of the cell culture bottle every 3 or 4 days.

2.6. Cell adhesion and spreading assay

Before testing, four different titanium specimens were washed with ethanol and distilled water, and disinfected by an autoclave before drying at 65 °C for 24 hours in an oven. To evaluate the morphology of cells grown on specimens, MC3T3-E1 cells (1 × 10^5 cells per well) were seeded on different specimens in 12-well culture plates. After culturing the cells for 4 hours, each specimen was washed using PBS and then fixed with 4% paraformaldehyde in PBS at room temperature for 10 minutes. Afterwards, each specimen was stained with Rhodamine Phalloidin (Cytoskeleton, USA) for 30 minutes at room temperature in the dark and then stained with 40,60-diamidino-2-phenylindole (DAPI) (Beyotime, Shanghai, China) for 30 seconds. The adherent cells in three random fields on each specimen were observed under a laser scanning confocal microscope (LSM710, Zeiss, GER). The cell number on each sample was counted at 200× magnification and the cell morphology was observed at 400× magnification.

2.7. Western blotting

The protein expressions of runt-related transcription factor 2 (Runx2) and osteopontin (OPN) on four different titanium specimens were analyzed by western blotting. After culturing cells (2 × 10^5 cells per well) on different specimens in 6-well plates for 7 and 14 days, the cells were rinsed with cold PBS and protein samples were harvested by lysis in RIPA buffer. The BCA protein assay kit (Key-GEN BioTECH, Nanjing, China) was used to determine total protein concentration. Protein extract samples (20 μg) were separated by electrophoresis and transferred to polyvinylidene fluoride (PVDF) membranes (Millipore, Billerica, MA, USA). The membranes were blocked with 5% skim milk for 1 hour at room temperature and then incubated with different primary antibodies against Runx2 (12556, CST, Beverly, MA, USA), OPN (ab8448, Abcam, USA), and β-actin (BM0627, Boster, Wuhan, China) overnight at 4 °C. Subsequently, the membranes were incubated with secondary antibodies (ZB-2301, goat anti-rabbit IgG; ZSGB-BIO, Beijing, China; AP124P, goat anti-mouse IgG; Millipore, USA) for 2 hours. Finally, the membranes were visualized *via* ECL western blot kit (Millipore, USA). The protein expressions of Runx2 and OPN were evaluated relative to that of β-actin as the internal control. The experiments were performed in triplicate.

2.8. Statistical analysis

The acquired data were analyzed using SPSS 22.0 software (SPSS Inc., Chicago, IL, USA). The Student's independent-samples *t*-test was used to compare differences in numerical results before and after immersion in *P. gingivalis* culture. The probability level for statistical significance was set at $\alpha = 0.05$.

3. Results

3.1. Surface observation and analysis

SEM images of different titanium specimens are shown in Fig. 1A. After 7 days of incubation with *P. gingivalis*, the Ti-pg and SLA-pg specimens were occupied by clusters of *P. gingivalis*, which formed a visible biofilm.

The representative XPS survey and high-resolution spectra of different titanium surfaces are exhibited in Fig. 1B. Ti and oxygen (O) were shown to be present on the titanium surfaces.

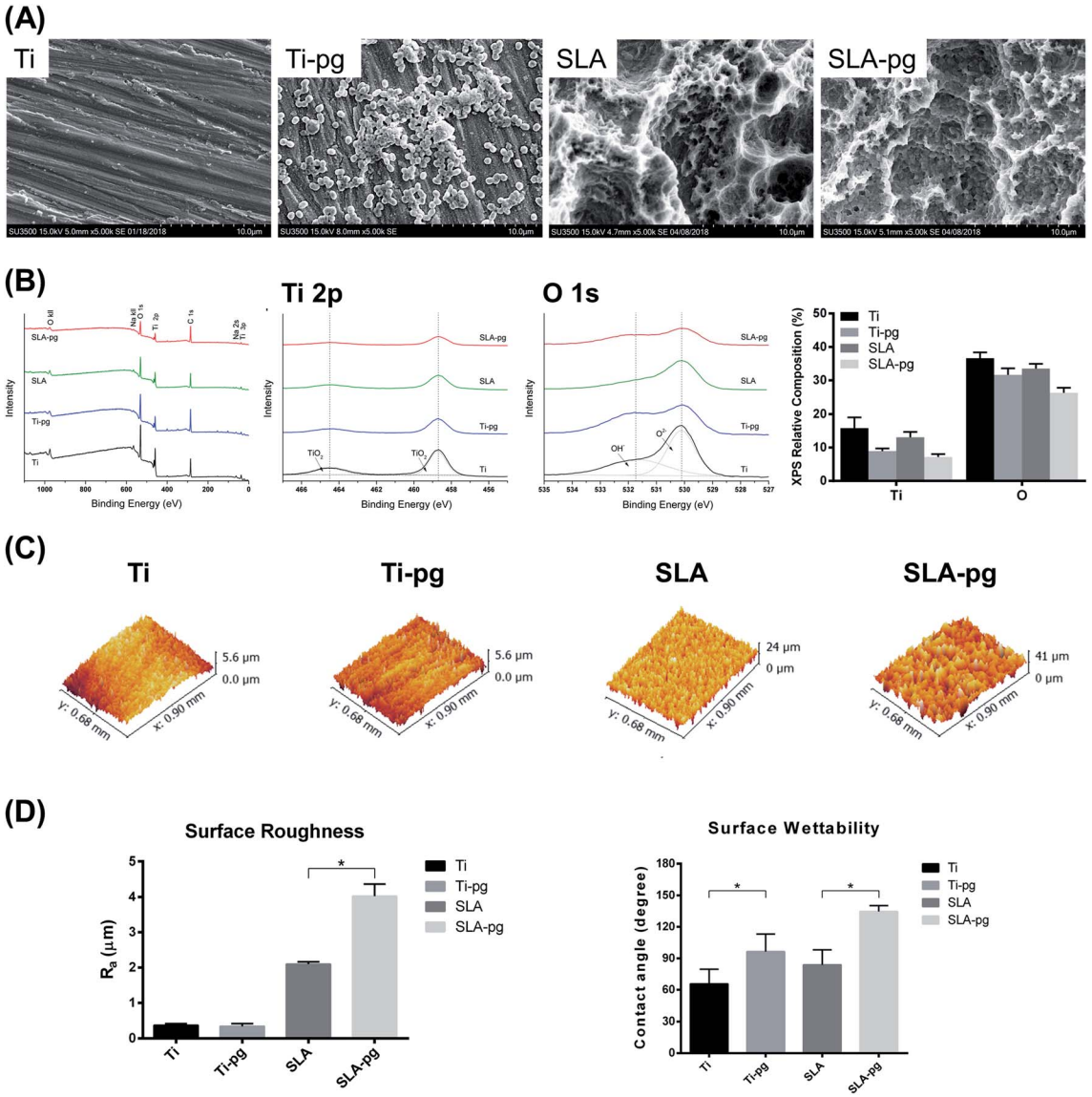

Fig. 1 Surface observation and analysis. (A) SEM images of pure and SLA titanium surfaces before and after immersion in *P. gingivalis* culture (magnification 5000×). (B) XPS survey spectra (Left), high-resolution spectra (Middle) of Ti 2p and O 1s, and relative composition of elements (Right) on pure and SLA titanium surfaces before and after immersion in *P. gingivalis* culture. (C) Three-dimensional topography of pure and SLA titanium surfaces before and after immersion in *P. gingivalis* culture. (D) Roughness values (Left) and contact angles (Right) of pure and SLA titanium surfaces before and after immersion in *P. gingivalis* culture (*$P < 0.05$).

Adventitious carbon (C) peaks originated from the laboratory environment. After immersing the metal in *P. gingivalis* culture for 7 days, both Ti 2p and O 1s peak intensities on the Ti-pg and SLA-pg surfaces decreased when compared to the control Ti and SLA surfaces. Moreover, from XPS high-resolution spectra analysis, the Ti 2p peaks, attributed to two symmetrical peaks at 458.8 eV (TiO_2) and 464.4 eV (TiO_2), revealed reductions on the Ti-pg and SLA-pg surfaces, which corresponded with decreases in their O 1s peaks at 530.1 (O^{2-}) and 531.8 eV (OH^-). The relative composition of Ti and O on the pure and SLA titanium surfaces before and after immersion in *P. gingivalis* culture are also compared in Fig. 1B. Both pure and SLA titanium surfaces revealed decreases in the level of Ti and O after incubation with the bacteria.

Fig. 1C and D presents the three-dimensional surface topography and surface roughness values of different specimens with and without immersion in medium containing *P. gingivalis*. The surface topography and roughness of Ti-pg specimen were similar to those of the control Ti specimen, whereas the surface of SLA-pg specimen became significantly rougher after being exposed to the bacteria ($P < 0.05$). The surface contact angles were also shown in Fig. 1D. According to the American Society for Testing and Materials (ASTM) D7334-08 specifications,[24] a surface is hydrophilic while the water contact angle is less than 45° and hydrophobic while the contact angle exceeds 90°. It was demonstrated that both Ti-pg and SLA-pg surfaces were more hydrophobic than the control Ti and SLA surfaces ($P < 0.05$).

3.2. Corrosion behavior

The representative EIS data of different groups are exhibited in the form of Nyquist plots, Bode phase and Bode $|Z|$ diagrams in Fig. 2. The Nyquist plots (Fig. 2A) showed that all specimens yielded data tracing a single semicircle. The diameters of the impedance loops of pure and SLA titanium specimens obviously decreased after immersing the metal in *P. gingivalis* culture, indicating less resistance to corrosion. At the lowest frequency of 0.01 Hz, as shown in Fig. 2B, the phase angles of Ti-pg and SLA-pg dropped to 74.3° and 81.3° respectively, which were lower than those of the control groups. As shown in Fig. 2C, the specimens of Ti-pg and SLA-pg exhibited lower values of the total impedance magnitude at the lowest frequency. The Bode phase and Bode $|Z|$ diagrams demonstrated that both pure and SLA titanium specimens with *P. gingivalis* exhibited lower impedance corresponding to corrosion resistance. As displayed in Fig. 2D, potentiodynamic polarization curves were constructed to show typical corrosion behaviors of the metal before and after immersion in *P. gingivalis* culture. The curves of Ti-pg and SLA-pg groups showed right-shifts, which indicated higher corrosion currents after exposure to the bacteria.

The spectra gained for all specimens were interpreted using an equivalent circuit model of $R_s(R_pQ)$, which is typical for the passive oxide layer.[25,26] In this model, R_s is on behalf of the electrolyte resistance, R_p is on the behalf of the corrosion resistance of surface oxide layer, and Q is on behalf of constant phase elements (CPE) of the inter-barrier layer. CPE, including Y_0 and n, means a shift capacitive behavior. The corresponding R_p, Y_0-CPE, n, and χ^2 values are listed in Table 1. The Chi-square value (χ^2) close to 10^{-3} indicated excellent consistency between the experimental data and fitting values. Learning from Table 1, the experimental Ti-pg and SLA-pg groups presented significant lower R_p and Y_0-CPE values ($P < 0.05$) than the control groups.

Moreover, the corrosion potential (E_{corr}), corrosion current (I_{corr}), and corrosion rate for different groups, as determined through potentiodynamic curves, are shown in Table 2. The E_{corr}, indicating the corrosion susceptibility, is the potential where the current density remarkably increases with increasing potential. According to the results in Table 2, both Ti-pg and

Table 1 Corrosion parameter values for pure and SLA titanium surfaces before and after immersion in *P. gingivalis* culture from EIS test[a]

	Impedance parameters ($n = 3$)			
Groups	R_p	Y_0-CPE	n	χ^2
Ti	2.24 (0.05)	5.18×10^{-5}	0.94	10^{-3}
Ti-pg	1.43 (0.17)*	4.16×10^{-5}*	0.87	10^{-3}
SLA	8.60 (1.48)	5.96×10^{-5}	0.95	10^{-3}
SLA-pg	6.65 (0.18)*	5.73×10^{-5}*	0.93	10^{-3}

[a] Values: mean (standard deviation); R_p (MΩ cm^{-2}); Y_0-CPE (μF cm^{-2}). *Indicates significant differences ($P < 0.05$) in the R_p and Y_0-CPE values between experimental (Ti-pg, SLA-pg) and control (Ti, SLA) groups.

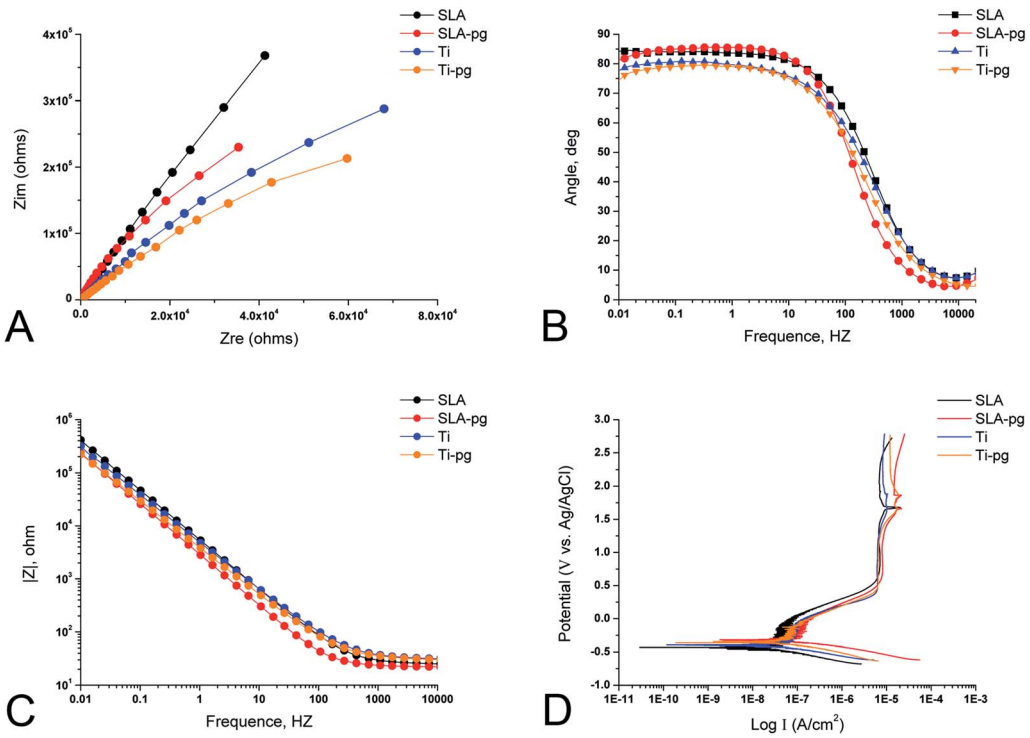

Fig. 2 Corrosion behavior of different titanium surfaces. (A) Nyquist plots for pure and SLA titanium surfaces before and after immersion in *P. gingivalis* culture. (B) Bode phase diagrams for pure and SLA titanium surfaces before and after immersion in *P. gingivalis* culture. (C) Bode $|Z|$ diagrams for pure and SLA titanium surfaces before and after immersion in *P. gingivalis* culture. (D) Potentiodynamic polarization curves for pure and SLA titanium surfaces before and after immersion in *P. gingivalis* culture.

Table 2 Corrosion parameter values of pure and SLA titanium surfaces before and after immersion in *P. gingivalis* culture from potentiodynamic polarization test[a]

	Corrosion parameters ($n = 3$)		
Groups	E_{corr}	I_{corr}	Corrosion rate
Ti	−0.32 (0.009)	1.23×10^{-8} (2.12×10^{-9})	1.45×10^{-4} (2.50×10^{-5})
Ti-Pg	−0.41 (0.003)*	2.26×10^{-8} (3.68×10^{-9})*	2.66×10^{-4} (4.33×10^{-5})*
SLA	−0.38 (0.075)	1.11×10^{-8} (6.25×10^{-10})	1.31×10^{-4} (7.34×10^{-6})
SLA-Pg	−0.35 (0.060)	1.55×10^{-8} (1.54×10^{-9})*	1.83×10^{-4} (1.82×10^{-5})*

[a] Values: mean (standard deviation); E_{corr} (mV); I_{corr} (μA cm^{-2}); corrosion rate (mm A^{-1}). *Indicates significant differences ($P < 0.05$) in the E_{corr}, I_{corr} and corrosion rate values between experimental (Ti-pg, SLA-pg) and control (Ti, SLA) groups.

SLA-pg groups exhibited decreases in E_{corr} values and statistical increases in values of I_{corr} and corrosion rate compared with the control Ti and SLA groups ($P < 0.05$). It demonstrated that the exposure to *P. gingivalis* did lead to more active corrosion behavior for the pure and SLA titanium.

3.3. Cell adhesion and spreading

Fig. 3A shows the number and morphology of MC3T3-E1 cells attached to different substrates after culturing for 4 hours. Measured by counting the cellular nuclei, the quantitative data revealed that there were significantly less adhered cells on the Ti-pg and SLA-pg substrates than those on the control pure and SLA titanium substrates ($P < 0.05$). Also, the cells extended less pseudopodia and spread less evenly across the pre-corroded Ti-pg and SLA-pg substrates.

3.4. Western blotting analysis

Western blotting analysis was used to explore the protein expression levels related to osteogenesis. As shown in Fig. 3B, MC3T3-E1 cells on the SLA-pg substrates expressed significantly less protein levels of Runx2 and OPN than those on the control SLA titanium substrate after culturing for 7 and 14 days. Although not statistical, the data revealed a decline in the protein expressions of Runx2 and OPN on the pure titanium substrate after the incubation with *P. gingivalis*.

4. Discussion

Based on the SEM, XPS, and EIS data, it was demonstrated that *P. gingivalis* colonization damaged the protective oxide film on pure and SLA titanium surfaces and induced electrochemical corrosion, which further negatively affected the osteoblast behavior according to the results of cell adhesion assay and western blotting analysis. Therefore, the research hypothesis was supported.

In this study, the *P. gingivalis* on pure and SLA titanium surfaces was observed by SEM. Our previous study has demonstrated that a bacterial biofilm could be formed on the pure titanium surface after incubation with *P. gingivalis* for 3 days and the culture medium changed from neutral to acidic.[27] Likewise, Souza *et al.*[23] reported the pH-lowering caused by microbial species on titanium specimens. Corrosion of titanium surface is prone to take place in the acid condition. Our SEM images confirmed that *P. gingivalis* could adhere, grow, and form microcolonies on pure and SLA titanium surfaces. *P. gingivalis* is recognized to produce acidic substances and proteases for their adhesion to and colonization on the metal surface. Moreover, other factors such as fimbriae, extracellular vesicles, or lipopolysaccharide may involve in the mechanism of attachment and a concomitant decrease in pH values.[28]

In the oral environment, titanium for dental applications depends on surface oxides for corrosion resistance.[29,30] After immersing the metal in the medium containing *P. gingivalis* in this study, the XPS survey spectra demonstrated an obvious decrease in the relative composition of Ti and O on the pure and SLA titanium surfaces when compared to the control groups. As shown in the XPS high-resolution spectra, it was further confirmed that the oxide layer formed on the outermost surface of the pure and SLA titanium was composed predominantly of TiO_2, which declined after exposure to *P. gingivalis*. This result was in agreement with some previous studies, which reported that bacteria could damage the titanium surface oxide layer.[22,27] It is well known that the natural oxide film on the titanium surface acts as a nonconductive barrier or resistor to electron flow between metal and an electrolyte to prevent the occurrence of biological corrosion.[31] Thus, the declined TiO_2 in surface oxides would weaken the oxide resistances of the pure and SLA titanium surfaces and hence their corrosion resistances. This was confirmed by the results of corrosion tests in the subsequent section of this study.

The surface roughness and wettability of the specimens were also altered after immersing the metal in *P. gingivalis* culture. The surface roughness of SLA-pg group significantly increased, compared to that of the control group of SLA, whereas the specimens of Ti and Ti-pg group revealed similar surface roughness. Barão *et al.*[19] reported that there was no significant difference in surface roughness between cpTi and Ti–6Al–4V alloy after the adhesion of *P. gingivalis* owing to their low roughness values, which agreed with our results. From the contact angle results, the two titanium surfaces, especially the SLA surface, became more hydrophilic, showing significant reductions in the wettability after exposure to *P. gingivalis*. Several studies demonstrated that the bacterial coating on titanium surface was roughness-dependent and its adhesion to

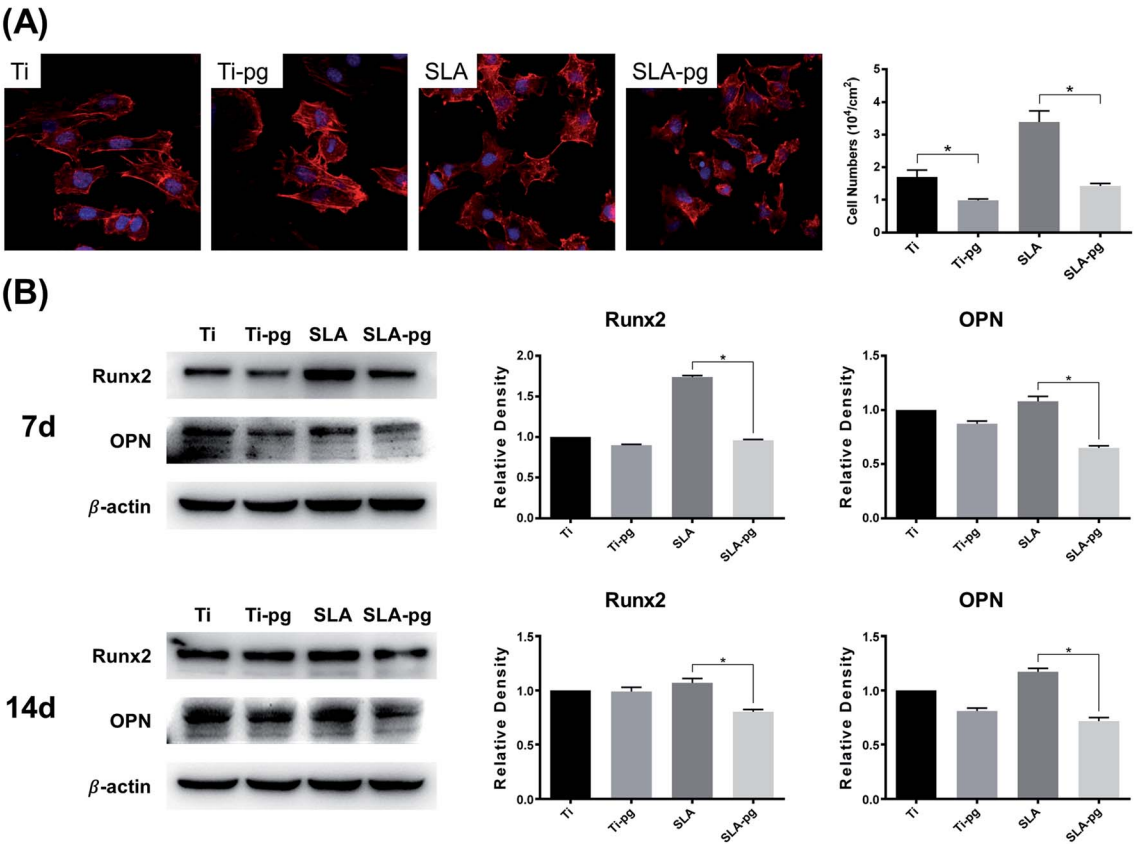

Fig. 3 Osteoblast behavior of MC3T3-E1 cells on different titanium surfaces. (A) Fluorescence images of MC3T3-E1 cells spreading (Left) on pure and SLA titanium surfaces before and after immersion in *P. gingivalis* culture after 4 hours of incubation (magnification 400×); quantitative analysis for the number of adherent MC3T3-E1 cells (Right) on different titanium surfaces (*$P < 0.05$). (B) Osteogenic-related protein expression levels of Runx2 and OPN of MC3T3-E1 cells (Left) on pure and SLA titanium surfaces before and after immersion in *P. gingivalis* culture detected by western blotting after 7 and 14 days of incubation; quantification for relative density of protein expression levels of Runx2 and OPN (Right), performed by Photoshop software (*$P < 0.05$).

the rougher SLA surface was significantly higher than the smooth surface.[32,33] In addition, as mentioned above, LPS and VSCs released form *P. gingivalis* could potentially promote titanium corrosion.[16] Thus, the higher degree of bacterial attachment, as well as the enhanced corrosion, may lead to more changes on the SLA titanium surface, including roughness and wettability.

The biocorrosion behavior on pure and SLA titanium surfaces caused by *P. gingivalis* was investigated by electrochemical techniques. As displayed in Fig. 2, the EIS spectra, including Nyquist plots, Bode phase and Bode $|Z|$ diagrams, combined with potentiodynamic polarization curves, gave a clear picture of the properties of the oxide films and corrosion behaviors of the studied titanium surfaces. After culturing with *P. gingivalis* for 7 days, the reduction of the impedance loop radius, as well as the decrease in impedance modulus, demonstrated the corrosive effect of *P. gingivalis* on both pure and SLA titanium specimens. The phase angles of Ti-pg and SLA-pg dropped to 74.3° and 81.3° at the lowest frequency of 0.01 Hz, respectively. A higher phase shift at lower frequency in Bode phase plots is indicative of a good passive film.[25,34] Thus, it was obvious that the passive film formed on both pure and SLA titanium specimens became defective or unstable after exposure to *P. gingivalis* for 7 days. The results were consistent with the above XPS results. Due to the weakening of passive films, the potentiodynamic polarization curves exhibited concomitant enhancing of corrosion currents for Ti-pg and SLA-pg specimens. These results were supported by corrosion parameter values shown in Table 1, the R_p of Ti-pg and SLA-pg was reduced to 1.43 and 6.65 MΩ cm^{-2}, which were significantly lower than that of the control pure and SLA titanium surfaces. Correspondingly, the potentiodynamic polarization curves showed active corrosion behaviors of the pure and SLA titanium specimens, which exhibited statistically higher values of I_{corr} and corrosion rate after incubation with *P. gingivalis* for 7 days. Therefore, together with the XPS analysis, the corrosion test results implied that the colonization of *P. gingivalis* could breakdown the oxide layers of pure and SLA titanium surfaces, resulting in weakened corrosion resistances and enhanced corrosion behaviors. Similar finding was also obtained with titanium exposed to oral biofilms composed of *S. mutans* and *C. albicans* using EIS and OCP tests.[23] It demonstrated that the presence of the oral biofilms decreased the titanium corrosion resistance and OCP, which indicated a tendency to corrosion.

The corroded titanium surface may lead to increasing bacterial attachment by oral pathogens.[19] The growth of microorganism and formation of biofilm on the titanium surface could produce a gel phase, as a diffusion barrier, and create concentration cells for metabolism with its byproducts, which could further enhance the biocorrosion.[35] Moreover, the biocorrosion of titanium could induce the release of titanium ions into surrounding environment. In our previous study, it was found that excessive titanium ions were capable of suppressing osteoblasts growth and inhibiting the osteogenic differentiation *via* the Hippo/YAP signaling pathway.[36]

Changes in the characteristics of titanium surfaces can directly influence cell adhesion behavior.[37,38] In this study, the decreased adherent MC3T3-E1 cells and poor cell spreading on the Ti-pg and SLA-pg surfaces were observed. This result confirmed that pure and SLA titanium surfaces pre-corroded by *P. gingivalis* negatively affected the adhesion and spreading abilities of osteoblasts. The osteogenic differentiation of cells on specimens was compared at the protein levels. Runx2 and OPN were chosen as significant osteogenic markers to analyze cell differentiation activities. Runx2 is a vital transcription factor for osteoblast differentiation which expressed in the early stage of osteogenic differentiation.[38] As a mediating marker for osteogenic differentiation, OPN is mainly related to osteoblast maturation in the relatively early stage.[39] The western blotting data clearly showed declined expressions of Runx2 and OPN on the two titanium surfaces. According to these results, the pure and SLA titanium surfaces pre-corroded by *P. gingivalis* could down-regulate osteogenic activity of osteoblasts, which might negatively affect the bone formation around the implants.

It is well known that hydrophilicity is regarded as the promoting factors for cell adhesion.[40,41] Toffoli *et al.*[42] reported that better hydrophilicity could improve the capacity of titanium to selectively adsorb fibronectin and fibrinogen, which was favorable for the attachment and proliferation of osteoblasts. A multitude of researches found that modified titanium surfaces with decreased contact angles had a potential to increase cell adhesion.[43–45] In our previous study, it was also confirmed that nanosheets modified titanium surface, which revealed superhydrophilicity, could dramatically enhance the cell adhesion and spreading.[38] Furthermore, preferential growth and matrix mineralization of osteoblasts have been observed on hydrophilic substrates.[40] As the first stage of interactions between cell and biomaterial, initial cell adhesion plays a key role in regulating the subsequent cell growth and differentiation.[46,47] In the present study, there were significantly less adherent cells on pre-corroded pure and SLA titanium surfaces, which should be attributed to the influence of worse hydrophilicity together with reduced protein adsorption ability. Both decreased initial number of adhesive cells and poor cell spreading on the titanium surfaces may have resulted in the observed attenuation of osteogenic differentiation as well.[46] Thus, it was believed that the significant reductions in the wettability of pre-corroded pure and SLA titanium surfaces contributed to the negative results of cell adhesion and spreading, which, in turn, led to the decline in the osteogenic activity of osteoblasts. Various factors, including bacterial colonization, surface roughness, wettability, chemical composition, and electrochemical corrosion behavior, may involved in the alterations of osteoblast behavior on the pure and SLA titanium surface in this work. However, the underlying mechanism in the biocorrosion of pure and SLA titanium surfaces in presence of *P. gingivalis* with metabolic byproducts as well as its regulation on the osteoblast behavior still requires further investigations.

5. Conclusions

P. gingivalis was able to colonize on the pure and SLA titanium surfaces and weaken their surface properties, especially a decrease in the protective TiO_2 film, which caused a decline in the corrosion resistance and further induced the biocorrosion. The pre-corroded pure and SLA titanium surfaces exhibited lower osteocompatibility and down-regulated the adhesion, spreading and osteogenic differentiation abilities of MC3T3-E1 cells.

Author contributions

All listed authors designed the study, performed the experiments and statistical analysis, and wrote the manuscript. All authors have read the manuscript and approved the final version.

Conflicts of interest

All authors declare that they have no conflicts of interest.

Acknowledgements

This work was supported by the National Natural Science Foundation of China (Project Number: 81870799), the Jiangsu Provincial Key Research and Development Program (Project Number: BE2019728), the Jiangsu Provincial Medical Youth Talent (Project Number: QNRC2016850), the Nanjing Medical University-SUYAN Group Intelligent Innovation Research and Development Project (Project Number: NMU-SY201806), the Southeast University-Nanjing Medical University Cooperative Research Project (Project Number: 2242017K3DN14), and the Foundation of Priority Academic Program Development of Jiangsu Higher Education Institutions (Project Number: 2018-87).

References

1 X. Chen, Q. Fu, Y. Jin, M. Li, R. Yang, X. Cui and M. Gong, *Mater. Sci. Eng., C*, 2017, **70**, 1071–1075.
2 T. H. Lin, H. T. Hu, H. C. Wang, M. C. Wu, S. W. Wu and M. L. Yeh, *PLoS One*, 2017, **12**, e0188364.
3 S. Lavenus, V. Trichet, S. Le Chevalier, A. Hoornaert, G. Louarn and P. Layrolle, *Nanomedicine*, 2012, **7**, 967–980.
4 K. Anselme, P. Davidson, A. M. Popa, M. Giazzon, M. Liley and L. Ploux, *Acta Biomater.*, 2010, **6**, 3824–3846.

5 J. Zhang, Y. Xie, J. Zuo, J. Li, Q. Wei, Z. Yu and Z. Tang, *Mater. Sci. Eng., C*, 2017, **78**, 1187–1194.
6 J. C. Souza, P. Ponthiaux, M. Henriques, R. Oliveira, W. Teughels, J. P. Celis and L. A. Rocha, *J. Dent.*, 2013, **41**, 528–534.
7 M. Lehnert, M. Gorbahn, C. Rosin, M. Klein, I. Koper, B. Al-Nawas, W. Knoll and M. Veith, *Langmuir*, 2011, **27**, 7743–7751.
8 M. Lewandowska, A. Roguska, M. Pisarek, B. Polak, M. Janik-Czachor and K. J. Kurzydlowski, *Biomol. Eng.*, 2007, **24**, 438–442.
9 B. J. Teubl, C. Schimpel, G. Leitinger, B. Bauer, E. Frohlich, A. Zimmer and E. Roblegg, *J. Hazard. Mater.*, 2015, **286**, 298–305.
10 M. H. Fathi, M. Salehi, A. Saatchi, V. Mortazavi and S. B. Moosavi, *Dent. Mater.*, 2003, **19**, 188–198.
11 K. Apaza-Bedoya, M. Tarce, C. A. M. Benfatti, B. Henriques, M. T. Mathew, W. Teughels and J. C. M. Souza, *J. Periodontal Res.*, 2017, **52**, 946–954.
12 G. E. Salvi, R. Cosgarea and A. Sculean, *J. Dent. Res.*, 2017, **96**, 31–37.
13 R. A. Gittens, R. Olivares-Navarrete, R. Tannenbaum, B. D. Boyan and Z. Schwartz, *J. Dent. Res.*, 2011, **90**, 1389–1397.
14 Y. C. de Waal, H. V. Eijsbouts, E. G. Winkel and A. J. van Winkelhoff, *J. Periodontol.*, 2017, **88**, 209–217.
15 V. Frojd, L. Chavez de Paz, M. Andersson, A. Wennerberg, J. R. Davies and G. Svensater, *Mol. Oral Microbiol.*, 2011, **26**, 241–252.
16 R. Harada, S. Takemoto, H. Kinoshita, M. Yoshinari and E. Kawada, *Mater. Sci. Eng., C*, 2016, **62**, 268–273.
17 M. Di Giulio, T. Traini, B. Sinjari, A. Nostro, S. Caputi and L. Cellini, *Clin. Oral Implants Res.*, 2016, **27**, 918–925.
18 M. Egawa, T. Miura, T. Kato, A. Saito and M. Yoshinari, *Dent. Mater. J.*, 2013, **32**, 101–106.
19 V. A. Barão, C. J. Yoon, M. T. Mathew, J. C. Yuan, C. D. Wu and C. Sukotjo, *J. Periodontol.*, 2014, **85**, 1275–1282.
20 A. Carlen, K. Nikdel, A. Wennerberg, K. Holmberg and J. Olsson, *Biomaterials*, 2001, **22**, 481–487.
21 S. Zhang, J. Qiu, Y. Ren, W. Yu, F. Zhang and X. Liu, *J. Mater. Sci.: Mater. Med.*, 2016, **27**, 78.
22 S. M. Zhang, J. Qiu, F. Tian, X. K. Guo, F. Q. Zhang and Q. F. Huang, *J. Mater. Sci.: Mater. Med.*, 2013, **24**, 1229–1237.
23 J. C. Souza, M. Henriques, R. Oliveira, W. Teughels, J. P. Celis and L. A. Rocha, *Biofouling*, 2010, **26**, 471–478.
24 American Society for Testing and Materials (ASTM), *D7334–08, Standard Practice for Surface Wettability of Coatings, Substrates and Pigments by Advancing Contact Angle Measurement*, ASTM International, West Conshohocken, PA, USA, 2013.
25 J. Qiu, W. Q. Yu and F. Q. Zhang, *J. Mater. Sci.*, 2011, **46**, 1359–1368.
26 M. Sharma, A. V. Kumar and N. Singh, *J. Mater. Sci.: Mater. Med.*, 2008, **19**, 2647–2653.
27 P. P. Ming, S. Y. Shao and J. Qiu, *Acta Univ. Med. Nanjing*, 2016, **10**, 1249–1253.
28 L. Badihi Hauslich, M. N. Sela, D. Steinberg, G. Rosen and D. Kohavi, *Clin. Oral Implants Res.*, 2013, **24**(Suppl A100), 49–56.
29 J. Qiu, W. Q. Yu, F. Q. Zhang, R. J. Smales, Y. L. Zhang and C. H. Lu, *Eur. J. Oral Sci.*, 2011, **119**, 93–101.
30 M. Bahraminasab, M. Bozorg, S. Ghaffari and F. Kavakebian, *Mater. Sci. Eng., C*, 2019, **102**, 200–211.
31 M. Metikos-Hukovic, Z. Pilic, R. Babic and D. Omanovic, *Acta Biomater.*, 2006, **2**, 693–700.
32 P. Bermejo, M. C. Sanchez, A. Llama-Palacios, E. Figuero, D. Herrera and M. Sanz Alonso, *Clin. Oral Implants Res.*, 2019, **30**, 725–734.
33 L. Rimondini, S. Fare, E. Brambilla, A. Felloni, C. Consonni, F. Brossa and A. Carrassi, *J. Periodontol.*, 1997, **68**, 556–562.
34 J. Qiu, C. B. Tang, Z. J. Zhu, G. X. Zhou, J. Wang, Y. Yang and G. P. Wang, *J. Mater. Sci.: Mater. Med.*, 2013, **24**, 2519–2528.
35 J. C. Chang, Y. Oshida, R. L. Gregory, C. J. Andres, T. M. Barco and D. T. Brown, *Bio-Med. Mater. Eng.*, 2003, **13**, 281–295.
36 W. Q. Zhu, P. P. Ming, J. Qiu, S. Y. Shao, Y. J. Yu, J. X. Chen, J. Yang, L. N. Xu, S. M. Zhang and C. B. Tang, *J. Appl. Toxicol.*, 2018, **38**, 824–833.
37 P. P. Ming, S. Y. Shao, J. Qiu, J. Yang, Y. J. Yu, J. X. Chen, W. Q. Zhu and C. B. Tang, *Appl. Surf. Sci.*, 2017, **416**, 790–797.
38 S. Y. Shao, P. P. Ming, J. Qiu, Y. J. Yu, J. Yang, J. X. Chen and C. B. Tang, *RSC Adv.*, 2017, **7**(11), 6753–6761.
39 S. Mohammadi, S. H. Ghaffari, M. Shaiegan, M. Nikogoftar Zarif, M. Nikbakht, K. Alimoghaddam and A. Ghavamzadeh, *Int. J. Hematol. Oncol. Stem Cell Res.*, 2016, **10**, 120–129.
40 W. Zhang, Z. Li, Y. Liu, D. Ye, J. Li, L. Xu, B. Wei, X. Zhang, X. Liu and X. Jiang, *Int. J. Nanomed.*, 2012, **7**, 4459–4472.
41 L. Ferreira, J. M. Karp, L. Nobre and R. Langer, *Cell Stem Cell*, 2008, **3**, 136–146.
42 A. Toffoli, L. Parisi, M. G. Bianchi, S. Lumetti, O. Bussolati and G. M. Macaluso, *Mater. Sci. Eng., C*, 2020, **107**, 110250.
43 B. Li, Y. Li, J. Li, X. Fu, H. Li, H. Wang, S. Xin, L. Zhou, C. Liang and C. Li, *J. Mater. Sci.: Mater. Med.*, 2014, **25**, 199–205.
44 X. Li, T. Chen, J. Hu, S. Li, Q. Zou, Y. Li, N. Jiang, H. Li and J. Li, *Colloids Surf., B*, 2016, **144**, 265–275.
45 T. Wang, Y. Wan and Z. Liu, *J. Mater. Sci.: Mater. Med.*, 2016, **27**, 133.
46 K. Anselme, *Biomaterials*, 2000, **21**, 667–681.
47 T. Miyauchi, M. Yamada, A. Yamamoto, F. Iwasa, T. Suzawa, R. Kamijo, K. Baba and T. Ogawa, *Biomaterials*, 2010, **31**, 3827–3839.

